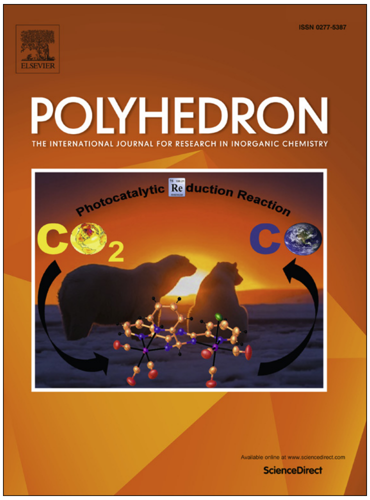

Synthesis and Crystal Structure of Cobalt (II) Schiff Base Precursor for Cobalt Oxide Thin Film by Thermal Chemical Vapor Deposition

P. Sravanthi, C. Chandrakala, M.G. Johnson, S. Arokiasamy, K.S. Nagaraja, B. Jeyaraj

PII: S0277-5387(15)00783-4
DOI: http://dx.doi.org/10.1016/j.poly.2015.12.033
Reference: POLY 11732

To appear in: *Polyhedron*

Received Date: 27 September 2015
Accepted Date: 17 December 2015

Please cite this article as: P. Sravanthi, C. Chandrakala, M.G. Johnson, S. Arokiasamy, K.S. Nagaraja, B. Jeyaraj, Synthesis and Crystal Structure of Cobalt (II) Schiff Base Precursor for Cobalt Oxide Thin Film by Thermal Chemical Vapor Deposition, *Polyhedron* (2015), doi: http://dx.doi.org/10.1016/j.poly.2015.12.033

Synthesis and Crystal Structure of Cobalt (II) Schiff Base Precursor for Cobalt Oxide Thin Film by Thermal Chemical Vapor Deposition

P. Sravanthi [a], C. Chandrakala [a], M. G. Johnson [a], S. Arokiasamy [b], K. S. Nagaraja [a], B. Jeyaraj [a*]

[a] Department of Chemistry, Loyola Institute of Frontier Energy (LIFE), Loyola College, Chennai – 34, India
[b] Department of Chemistry, VIT University, Chennai – 127, India
[*]Corresponding author. Tel.:+91 8056029860
E-mail: psravanthireddy1@gmail.com, Jeyaraj.boniface@gmail.com

Abstract

The tetrahedral Schiff base complex bis(N-isopropylsalicylaldimine)cobalt(II) [Co(saliprn)$_2$] (CSI) was prepared by template method. The complex was characterized by FT-IR, mass spectroscopy, TG/DTA and single crystal X-ray structure determination analysis. The dynamic TG analysis showed that the complex is completely volatile. The equilibrium vapor pressure of the complex was studied by non-isothermal and isothermal thermogravimetric transpiration techniques over the temperature range of 474 K – 514 K. The E_a (48.4 kJmol^{-1}) and ΔH_{sub} (111.54 kJmol^{-1}) for the complex and expression for temperature dependence of vapour pressure (P_e) obtained. The thermal behavior of the cobalt(II) complex was studied by thermogravimetry techniques using different non-isothermal heating rates under nitrogen atmosphere. The complex was found to be volatile and used in thermal chemical vapour deposition for the development of nanocrystalline cobalt oxide thin films over silica substrates. These nanocrystalline thin films were analyzed by XRD and SEM confirmed the presence of Co_3O_4 phase with almost nil carbon.

Keywords: Cobalt complex; thermo gravimetric analysis; Vapor pressure and kinetics; Cobalt Oxide Thin films; SEM and XRD.

1. Introduction:

Metal oxide thin films have attracted a lot of attention due to their importance in the material science, microelectronics, heterogeneous catalysis and also utilized as spacer layers on electrotransparent model systems [1-5]. The inorganic materials are formed from molecular metal-organic precursors by chemical vapor deposition, molecular beam epitaxy and sol-gel have advantages over solid-state synthesis [6]. The majority of the chemical vapor deposition activity has focused on fabrication of cobalt oxide thin film layers for magento-optic applications, electrochemical transparent properties of semiconducting oxides, strong electron interactions in solids, glass industry for colouration, and chemical process as catalytic activator in oxidation sites [7-10].

Chemical vapor deposition requires the metal complexes which should meet general conditions such as sublime without decomposition, easy handling, low or no toxicity for the material deposited and/or the substrate used [11]. The vapor pressure of the precursor as a function of temperature influences the choice of precursor in chemical vapor deposition and related processes [12]. Several techniques such as ebulliometric, static, manometric measurement and Knudsen cell techniques are currently used for the measurement of the vapor pressure of a pure substance [13, 14]. Several studies [15] have shown that thermogravimetry is a rapid and convenient technique for the determination of vapor pressure curves, enthalpy of sublimation and vaporization, solid state kinetics of chemical reactions for volatile compounds. Among several methods for vapor pressure measurements transpiration technique also known as gas-entertainment technique is more versatile and enables vapor pressure over a wide range of temperature [16]. Thermochemical properties of Schiff bases have attracted our attention in their ability to coordinate metal ions, acting as bidentate or tetradentate ligand to give metal chelates [17].

We hereby report the reaction of Schiff base ligands with Co^{2+} which led to potential precursors for producing cobalt oxide thin films for technological applications [18] by thermal chemical vapour deposition technique. This includes synthesis, crystal structure determination and thermogravimetric analysis. The differential and integral iso-conversional methods [17] were used for the evaluation of the activation energy from non-isothermal data. The vapor pressure of bis(N-isopropylsalicylaldimine)cobalt(II) was measured by thermogravimetry based transpiration technique [19, 20].

2. Experimental:

2.1.Materials:

Cobalt acetate tetrahydrate [Merck, 97%], and isopropylamine [Aldrich, 98%] were used as such in the synthesis of cobalt complexes. Methanol, acetone, dichloromethane and ethanol were used after distillation.

2.2.Synthesis of bis(N-isopropylsalicylaldimine)cobalt(II):

An ethanolic solution of salicylaldehyde (6 moles) and isopropyl amine (6 moles) were added to the aqueous solution of cobalt(II) acetate (7 moles) with constant stirring which was refluxed for 3-4 h at 323K and left for overnight in an ambient temperature. The obtained brick red precipitate was filtered and dried in a vacuum desiccator containing fused calcium chloride. The compound was recrystallised using dichloromethane which forms hexagonal crystals (Fig: 1) and dried over fused calcium chloride.

2.3.Characterization techniques:

The FT-IR spectrum for the complexes was recorded in KBr medium to infer the various stretching frequencies using Perkin Elmer FTIR spectrometer in the range of 4000-400 cm^{-1}. The Electronic Ionization - Mass Spectrum (EI-MS) was recorded by YOKUDELNA_ES+_2000 model at an accelerating voltage of 32V at ambient temperature. The thermogram was carried out with Perkin Elmer Pyris-Diamond TG-DTA. The purge gas was high purity nitrogen dried by passing through refrigerated molecular sieves (Linde 4A) at a flow rate 12 dm^3h^{-1}. The single crystal XRD data was collected using a Bruker Apex – II CCD diffractometer with omega and phi scan mode with Mo-Kα (λ=0.71073 Å) radiation at room temperature (T=296.3 K). The ORTEP view of the molecule was drawn at 50% probability thermal displacement ellipsoids with the atom numbering scheme. SEM for the cobalt oxide thin films was analysed by FEI Quanta FEG 200 instrument. The powder X-Ray diffraction measurements were performed with Bruker XPERT-PRO Spectrometer with a copper tube (λ=1.54060 Å).

2.4.Preparation of Thin film:

The thin films of cobalt oxide were coated by using the atmospheric thermal metallo-organic chemical vapour deposition (TMOCVD) where alumina served as a deposition chamber. Prior to each deposition, the silica substrate was sonicated for 30 min on an ultrasound sonicator and the reaction chamber was cleaned by acetone. This process was done to ensure that the deposition surfaces were free from contamination and defects.

For the deposition of cobalt oxide thin film, the cleaned surface of silica substrates and fine powder of the precursor were kept in a quartz boat which was kept in a working chamber.

This chamber was maintained at 550°C in a digitally controlled furnace. On getting to the hot zone, the precursor kept in the quartz boat sublimed before it thermally decomposed resulting in the coating on the substrates. The whole process was left for 2 h at the deposition temperature of 550°C. After cooling, the coated films were characterized by SEM/EDAX and XRD to analyze the phases.

3. Result and discussion:

3.1.Characterization:

The IR spectral studies (Fig: 2) suggested the band at 1605 cm^{-1} correspond to υ(C=N) upon complexation indicating the involvement of azomethine groups in the coordination and the band at 1330 cm^{-1} due to υ(phenolic C-O). The bands observed at 426 cm^{-1} and 528 cm^{-1} were assigned to υ(Co-N) and υ(Co-O) respectively [21]. The isotopic cluster peaks of the complex (Fig: 3) at m/z =384 is identified as the molecular ion peak. The cluster peaks at m/z=222 correspond to the species including metal. The peak at m/z = 164 corresponds to the ligand without the metal atom. The stereochemistry of the Co(II) complex was given by the magnetic moment 3.87 BM corresponding to three unpaired electrons which suggests four co-ordinate tetrahedral arrangement.

3.2.Non-Isothermal Thermogravimetry (TG) study:

Bis(N-isopropylsalicylaldimine)cobalt(II) complex undergoes single smooth step weight loss on heating between 474 - 514 K with nil residue (Fig:4). It is interesting to note that the enhanced thermal stability and volatility is due to expulsion of two water molecules and coordination of azomethine nitrogen (-CH=NH) with Co instead of carbonyl oxygen as in bis(salicylaldehydato)cobalt(II) dihydrate. It was decided to substitute H of =NH (Fig: 1) by alkyl chains thereby tuning the volatilization behavior depending upon the length of the alkyl chain. The single step weight loss gives a wide temperature window for volatilization as the melting point is the important requirement for potential precursor for CVD applications [22, 23].

Non-isothermal TG runs of CSI at different heating rates revealed that the complex was thermally stable upto 514 K. The temperature dependent equilibrium vapor pressure derived from Dalton's law of partial pressures for a mixture of ideal gas is calculated as:

$$P_e = WRT_c/MV_C$$

Where W is the mass loss at various isothermal temperatures, V_c is the flow of carrier gas, R is the universal gas constant, M is the molecular mass of the monomeric precursor vapor species, T_c is the temperature of the carrier gas. The vapor pressure P_e at each saturation temperature was calculated from the mass loss of the sample within a definite period. Attainment of equilibrium conditions was evident from the mass loss plots at all the isothermal steps as seen from the straight line plots passing through the origin (Fig: 5a), showing equal masses are vaporized in equal intervals of time. The least-square expressions for the complex derived from the corresponding vapor pressure data plotted as log P_e vs 1/T (Fig: 5b) .The temperature dependence of P_e could be represented by the expression

$$\ln\left(\frac{P_e}{mPa}\right) = \frac{-58{,}284 \pm 981}{\frac{T}{K}} + 18 \pm 0.2\ (474 - 514K)$$

The enthalpy of vaporization was calculated by multiplying the slope of the equation with -2.303 R, a value of 111.54 K J mol^{-1} was derived for the standard enthalpy of sublimation ($\Delta_{sub}H$) [15, 24, 25].

3.3.Determination of activation energy:

The rate constant k for the vaporization enthalpy of the complexes was determined for every 10 % weight loss of the complex. The expression for k is given by

$$k = \frac{d\alpha}{dt}$$

Where dα/dt is the derivative of the fraction vaporized with respect to time and k is the rate constant of vaporization, whereas degree of conversion (α) is calculated in terms of mass loss.

$$\alpha = \frac{w_i - w_t}{w_i - w_f}$$

Where w_t is the weight at any time, w_i and w_f are the initial and final weights. The Arrhenius expression is represented as

$$k = Ae^{\frac{-E_a}{RT}}$$

The plot of ln k versus 1000/T (Fig: 6a) was found to be linear. The activation energy (E_a) for the vaporization of the complexes was calculated from the slope. The activation energy values for different heating rates of 2, 4, 6, 8, 10 and 12 K $min^{-1}$are obtained as 111±0.4, 110±0.4, 109±0.4, 113±0.4, 116±0.4 and 115±0.4 $kJmol^{-1}$. However, due to complexity of the kinetic description concerning the solid state reaction processes, it is usually assumed that the apparent activation energy is not a constant value but depends on α. Therefore, the kinetic procedure adopted in this work was first based on two multi-heating rate methods. Both approaches determine the activation energy using thermal analysis data carried out at different fixed heating rates. The activation energy for the non-isothermal sublimation of CSI was calculated using Kissinger expression:

$$\ln\left[\frac{\beta}{T_m^2}\right] = ln\left[\frac{n(1-\alpha_m)^{n-1}AR}{E_a}\right] - \left[\frac{E_a}{RT_m}\right]$$

Where T_m and α_m are the absolute temperature and weight loss at the maximum weight-loss rate $(d\alpha/dt)_m$. From the slope of $\ln(\beta/T^2_m)$ against $1/T_m$ (Fig: 6b) the activation energy was found to be 123±1$kJmol^{-1}$. The activation energy values for different conversion levels were also determined by Flynn-Wall-Ozawa technique [26] with the expression:

$$ln(\beta) = ln\left[\frac{AE_a}{R}\right] - ln[F(\alpha)] - \frac{E_a}{RT}$$

The straight lines obtained from the plots of heating rates against temperature (Fig: 6c) gave a mean E_a value 107±0.7$kJmol^{-1}$. Kissinger-Akahira-Sunrose method [27, 28] similar to Kissinger method, but thermodynamic temperature for the maximum weight loss was replaced by thermodynamic temperature adequate for a certain level of conversion of the complex is expressed by the equation as

$$ln\left[\frac{\beta}{T^2}\right] = ln\left[\frac{AR}{Eg(x)}\right] - \frac{E}{RT}$$

The plot $\ln(\beta/T^2)$ against 1/T (Fig: 6d) gave a straight line with apparent activation energy as 98±0.7 $kJmol^{-1}$. The activation energy by Friedman method (Fig: 6e) [29] from the following expression yielded a value 93.8±1.3 $kJmol^{-1}$.

$$ln\left[\beta\left(\frac{d\alpha}{dT}\right)\right] = ln[Af(\alpha)] - \frac{E_a}{RT}$$

The model fitting analysis of the non-isothermal data (Table 1) suggest that the sublimation kinetics follow the models. The experimentally determined value suggests that the thermal signification occurs predominantly via congruent sublimation as a single step process.

3.4.Structural description of Compound:

The crystal structure was solved by a direct method with the SHELXS- 97 program [29, 30]. The single crystal data (Table 2) of the bis(N-isopropylsalicylaldimine)cobalt(II) complex (CCDC No: 1012524) revealed that it crystallizes in the orthorhombic space group *Pbac*. The unique metal center (Co) is surrounded by two Schiff base ligands (Fig.7) forming a distorted tetrahedron. The ligand is bidentate with one phenolato – O and one imine – N as the donor sites. The basal plane of the cobalt(II) is formed by two imine nitrogen and two phenolato oxygen atoms which are in the axial positions from the two Schiff base ligands giving CoN_2O_2, with exception of the isopropyl groups the complex shows almost perfect C_2 symmetry. The bond lengths (Table 3) of C(7) – N(1) [1.289Å] and C(17) – N(2) [1.272 Å] confirm the presence of double bonds and are comparable to those in other Schiff base complex [31]. The co-ordination of the nitrogen to the cobalt metal caused the reduction of bond lengths of Co(1) – O(1)[1.9020 Å] of the isopropyl substituted complex from 1.921Å in the parent compound $Co(sal)_2$. The co-ordination by nitrogen which replaces oxygen in $Co(sal)_2$ increased the covalent nature and volatility. The bond angle Co(1) – N(2) – C(17) is 120.69°and the rotational motion of the alkyl groups shield the cobalt atom from the approach of water molecule [32].

3.5.Scanning Electron Microscope and EDAX of cobalt oxide coated thin films:

The cobalt oxide thin films were prepared by atmospheric thermal CVD method on silica substrate using the present complex as MOCVD precursor. The surface morphology of the thin film (Fig: 8) was determined by the rate of precursor transport, decomposition reaction, surface diffusion and lattice incorporation during the deposition process. The surface morphology of the deposited films revealed a progressive grain growth with increasing temperature. The SEM micrographs of cobalt oxide films exhibit uniform dense microstructure grown at 550 °C over silica substrate. Energy Dispersion X-Ray (EDX) analysis was carried out on as deposited cobalt oxide films indicating the peaks corresponding to cobalt and oxygen. No sizeable carbon contamination could be detected supporting the purity of the film by thermal chemical vapour deposition. In our previous work, the deposition of CrN/Ni by Plasma Assisted Metallo Organic CVD using precursors like $[Cr(acac)_3]$ and $[Ni(acac)_2en]$ small amounts of carbon deposition was observed. This was rectified by using certain catalysts like ammonium biflouride [33]. In the present work EDAX indicated the absence of carbon.

The powder cobalt oxide from thin films deposited at 550 °C on a Si(100) substrate have shining blackish grey colour which was found to be crystalline with (311) orientation (JCPDS No 78:1969) revealing the presence of face centered cubic plane by powder XRD. It was observed that the films deposited in the oxygen atmosphere comprised of Co_3O_4 phase without carbon contamination. The detection limit for carbon is greater than 5% in XRD. According to the XRD data (311) is the strongest reflection in the polycrystalline Co_3O_4, being as strong as (111) reflection. The preference for (111) over (220) and (400) is also observed (Fig: 9). XRD study of the crystallite reduced form of different cobalt oxides have been investigated by X-Ray diffraction and the peaks indexed for each type of cobalt oxide [34]. Cobalt oxide thin films have also been developed using $Co(acac)_3$ as MOCVD precursor and obtained CoO an Co_2O_3 phases under N_2 atmosphere with slight amount of carbon [10]. In the present study as it being atmospheric chemical vapour deposition we obtained Co_3O_4 as a major phase and no CoO phase could be detected. The average grain size of the powder Co_3O_4 obtained from the thin film deposition was calculated using Debye-Scherrer's equation.

$$D = \frac{0.9\lambda}{w \cos\theta}$$

Where D is the grain size, λ is the x-ray wavelength, θ is the Bragg angle, w is the full width at half maximum of diffraction peak. The average grain size is observed at 5.89 nm at lattice constant of 5.17 Å [35].

4. Conclusion:

The coordination complexes of several transition metals have been extensively used as precursors for the production of the metallic or metal oxide films by TCVD process. Hence a systematic approach for the development of volatile precursor using aromatic based ligand resulted a promising vapour source of cobalt. This complex is a better precursor for thermal CVD owing to the high volatility of imine (-CH=NH) based complex. The vapor pressure (P_e) and sublimation enthalpies (ΔH_{sub}) were evaluated for bis(N-isopropylsalicylaldimine)cobalt(II) complex by TG based transpiration technique in which activation energy was found to agree with enthalpy of isothermal sublimation process. The activation energy values for non-isothermal sublimation processes agree with each other. The SEM images confirm the uniform coating of the complex over silica substrate, with the incorporation of cobalt and oxygen with almost nil carbon residues.

Supplementary material

Crystallographic data of bis(N-isopropylsalicylaldimine)cobalt(II) complex has been deposited with the Cambridge Crystallographic Data Centre [CCDC No. 1012524]. Copies of the data can be obtained free of charge at www.ccdc.cam.ac.uk/conts/retrieving.html or from the Cambridge Crystallographic Data Centre (CCDC), 12 Union Road, Cambridge CB2 1EZ, UK; fax: +44 0 1223 336 033; email: deposit@ccdc.cam.ac.uk.

5. References:

[1]. H.M. Benia, P. Myrach, N. Nilius, H. J. Freund, Surf. Sci. 604(2010) 435-441.

[2]. M. Bäumer, H.-J. Freund, Progr. Surf. Sci. 61 (1999) 127-198.

[3]. S. A. Chambers, Surf. Sci. Rep. 39 (2000) 105-180.

[4]. C. T. Campbell, Surf. Sci. Rep. 27 (1997) 1-111 .

[5]. W. Weiss, W. Ranke, Prog. Surf. Sci. 70 (2002) 1-151.

[6]. M. Hamid, A. A. Tahir, M. Mazhar, K. C. Molloy, G. Kociok-Kohn, Inorg. Chem. Commun. 11 (2008) 1159-1161.

[7]. N.D. Papadopoulos, E. Illekova, H. S. Karayanni, E. Hristoforou, J. Optoelectron. Adv. Mater. 10 (2008) 1098-1102.

[8]. A. R. Ivanova, G. Nuesca, X. Chen,C. Goldberg, A. E. Kaloyeros, B. Arkles, J. J. Sullivan, J. Electrochem. Soc. 146(2009) 2139-2145.

[9]. P. A. Lane, P. E. Oliver, P. J. Wright, C. L. Reeves, A. D. Pitt, B. Cockayne, Chem. Vap. Depos. 4(1998) 183-186.

[10]. C. U. Mordi, M. A. Eleruja, B. A. Taleatu, G. O. Egharevba, A. V. Adedeji, O. O. Akinwunmi, B. Olofinjana, C. Jeynes, E. O. B. Ajayi, , J. Mater. Sci. Technol. 25 (2009) 85-89.

[11]. M. Urrutigoity, C. Cecutti, F. Senocq, J. P. Gorrichon, A. Gleizes, Inorg. Chim. Acta. 248 (1996) 15-21.

[12]. T. Ohta, F. Cicoira, P. Doppelt, L. Beitone, P. Hoffmann, Chem. Vap. Depos. 7 (2001) 33-37.

[13]. F. Barontini, V. Cozzani, Thermochim. Acta. 460 (2007) 15-21.

[14]. P. Phang, D. Dollimore, Thermochim. Acta. 367-368 (2001) 263-271.

[15]. R. Pankajavalli, C. Mallika, O. M. Sreedhan, V. S. Raghunathan, P. Antony Premkumar, K. S. Nagaraja, Chem. Eng. Sci. 57 (2007) 3603-3610.

[16]. J. Selvakumar, D. Sathiyamoorthy, K. S. Nagaraja, Mater. Chem. Phys. 129 (2011) 62-67.

[17]. M. D. M. C. Ribeiro da Silva, J. M. Goncalves, A. L. R. Silva, A. M. R. O. A. Silva, P. C. F. C. Oliveira, M. A. V. Ribeiro da Silva, Thermochim. Acta. 420 (2004) 67-71.

[18]. V. Jeseentharani, J. Selvakumar, B. Varghese, A. Dayalan, K. S. Nagaraja, Adv. Mat. Lett. 4(2013) 643-649.

[19]. P. Budrugeac, D. Homentcovschi, E. Segal, J. Therm. Anal. Calorim. 66 (2001) 557-563.

[20]. M. Maria, J. Selvakumar, V. S. Ragunathan, Tom Mathews, K. S. Nagaraja, Thermochim. Acta. 2008, 474, 87-96.

[21]. A. A. Nejo, G. A. Kolawole, A. O. Nejo, J. Coord. Chem. 63 (2010) 4398-4410.

[22]. M. G. Johnson, J. Selvakumar, K. S. Nagaraja, Thermochim. Acta. 495 (2009) 38-41.

[23]. T. S. Arul Jeevan, Tom Mathews, V. S. Raghunathan, K. S. Nagaraja, Thermochim. Acta. 478 (2008) 41-44.

[24]. M. Maria, J. Selvakumar, V.S. Ragunathan, K. S. Nagaraja, Surf. Coat. Tech. 204 (2009) 222-227.

[25]. T. S. Arul Jeevan, S. Arokiasamy, T. Mathews, V. S. Raghunathan, K. S. Nagaraja, Mater. Lett. 62 (2008) 4170-4172.

[26]. M. F. G. Johnson, T. S. Arul Jeevan, S. Arokiasamy, K. S. Nagaraja, Am. J. Anal. Chem. 6 (2015) 118-126.

[27]. M. Kaleem Baloch, M. Jehan Zeb Khurram, G. Fatima Durrani, J. Appl. Polym. Sci. 120(2011) 3511-3518.

[28]. S. Vecchio, R. Di Rocco, C. Ferragina, Thermochim. Acta. 467(2008) 1-10.

[29]. J.Selvakumar, D.Sathyamoorthy, K.S.Nagaraja, Mater. Chem. Phys. 129 (2011) 62-67.

[30]. M.N. Burnett, C.K. Johnson, Acta Crystallogr. Sec.A. 52(a1) (1996) C93-C93.

[31]. G.M. Sheldrick, Acta Crystallogr. Sec.A. 64 (2008) 112–122.

[32]. D. Durak, A. Delikanli, C. Demetgul, I. Kani, S. Serin, Transit. Metal. Chem. 38 (2013) 199-206.

[33]. S. Arokiasamy, M.G. Johnson, C. Mallika, O. M. Sreedharan, K. S. Nagaraja, Mater. Chem. Phys. 114 (2009) 456-461.

[34]. P. Antony PremKumar, A. Dasgupta, P. Kuppusami, P. Parameswaran, C. Mallika, K. S. Nagaraja, V. S. Raghunathan, Chem. Vap. Depos. 12 (2006) 39-45.

[35]. O. A. Bulavchenko, S. V. Cherepanova, V. V. Malakhov, L. S. Dovlitova, A. V. Ishchenko, S. V. Tsybulya, Kinet. Catal. 50 (2009) 192-198.

[36]. A.U. Mane, S. A. Shivashankar, J. Cryst. Growth. 254(2003) 368-377.

Figure Titles:

1. Fig 1: Reaction Scheme of bis(N-isopropylsalicylaldimine)cobalt(II)
2. Fig 2: FT-IR spectrum of bis(N-isopropylsalicylaldimine)cobalt(II)
3. Fig 3: EI-Mass spectrum of bis(N-isopropylsalicylaldimine)cobalt(II)
4. Fig 4: TG/DTA of bis(N-isopropylsalicylaldimine)cobalt(II) in N_2 atmosphere at a heating rate of 10°C mi^{n-1}.
5. Fig 5: (a) Mass loss against time isothermal plots and (b) Clausius-Clapeyron plot.
6. Fig 6: Non-isothermal plots (a) Arrhenius Plots of ln k vs 1/T (b) Kissinger Plot of $\ln(\beta/T^2_m)$ vs $1/T_m$ (c) Flynn – Wall of ln β vs 1/T (d) Kissinger-Akahira-Sunrose (KAS) Plot of $\ln(\beta/T^2)$ vs 1/T (e) Friedman Plots of $\ln\beta^*(d\alpha/dT)$ vs 1/T of bis(N-isopropylsalicylaldimine)cobalt(II) at different heating rates (°C min^{-1}).
7. Fig 7: ORTEP and packing diagram of bis(N-isopropylsalicylaldimine)cobalt(II) with 50% probability.
8. Fig 8: SEM and EDAX images of the cobalt oxide coating obtained on silica substrate using bis(N-isopropylsalicylaldimine)cobalt(II) complex as precursor.
9. Fig 9: X-ray Diffraction of the powder cobalt oxide collected from the thin film coatings over silica substrate.

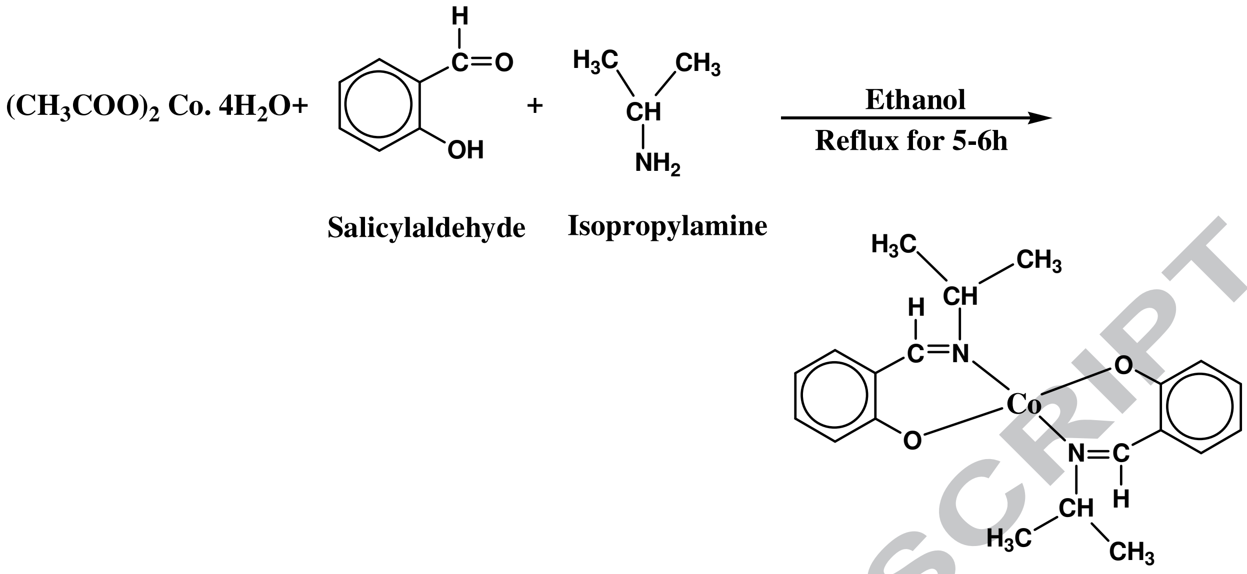

Fig 1: Reaction Scheme of bis(N-isopropylsalicylaldimine)cobalt(II)

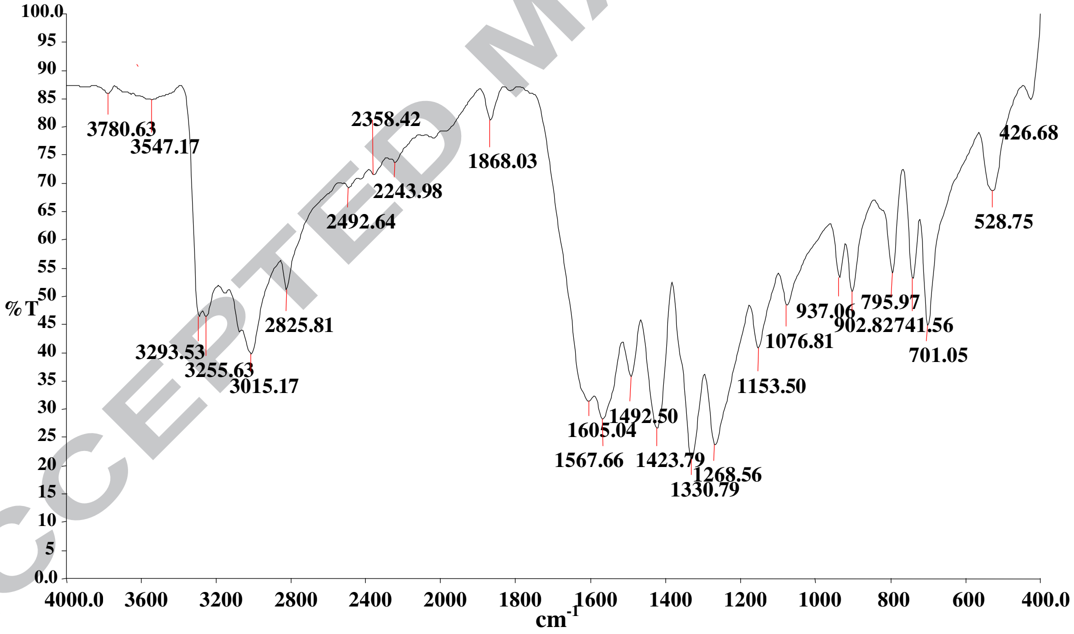

Fig 2: FT-IR spectrum of bis(N-isopropylsalicylaldimine)cobalt(II)

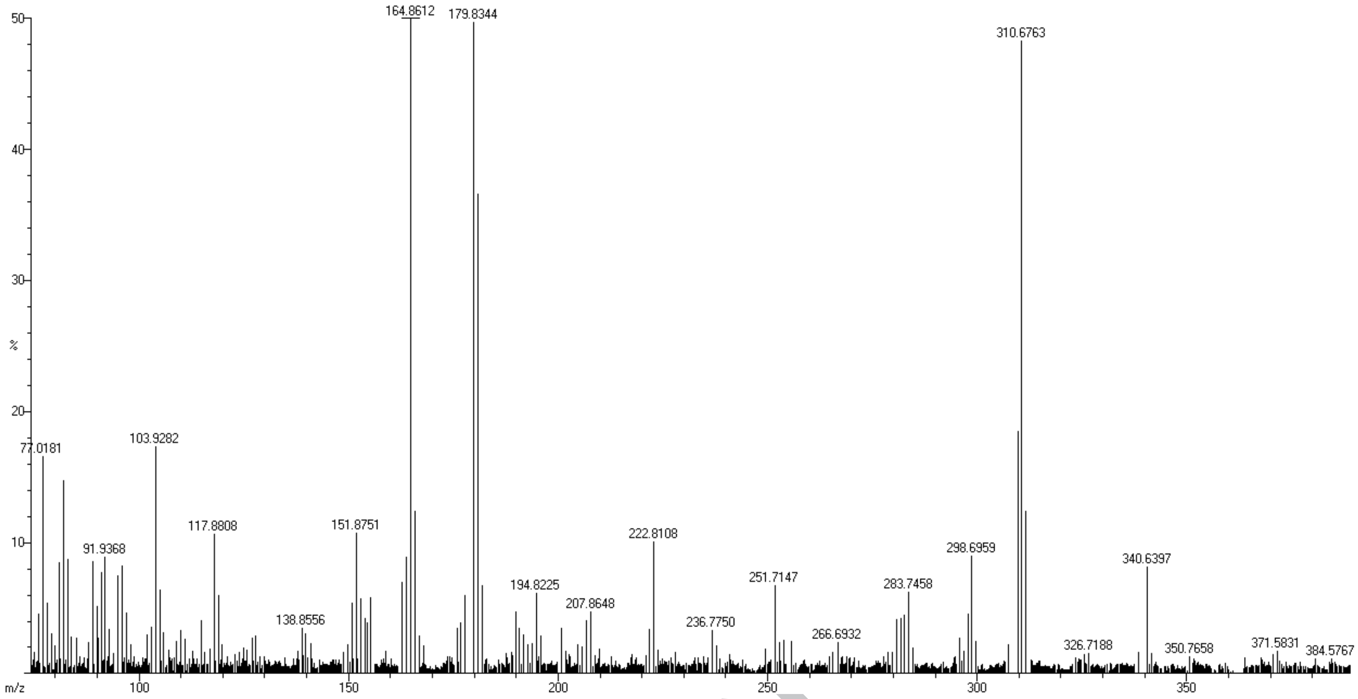

Fig 3: EI-Mass spectrum of bis(N-isopropylsalicylaldimine)cobalt(II)

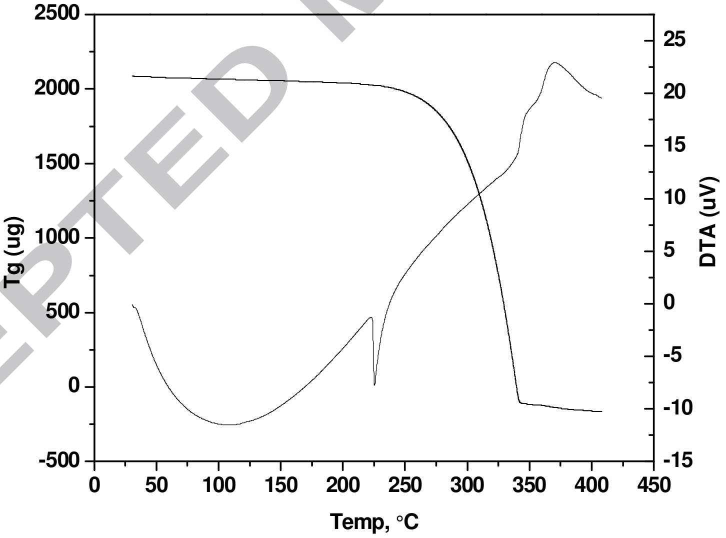

Fig 4: TG/DTA of bis(N-isopropylsalicylaldimine)cobalt(II) in N_2 atmosphere at a heating rate of 10°C min^{-1}

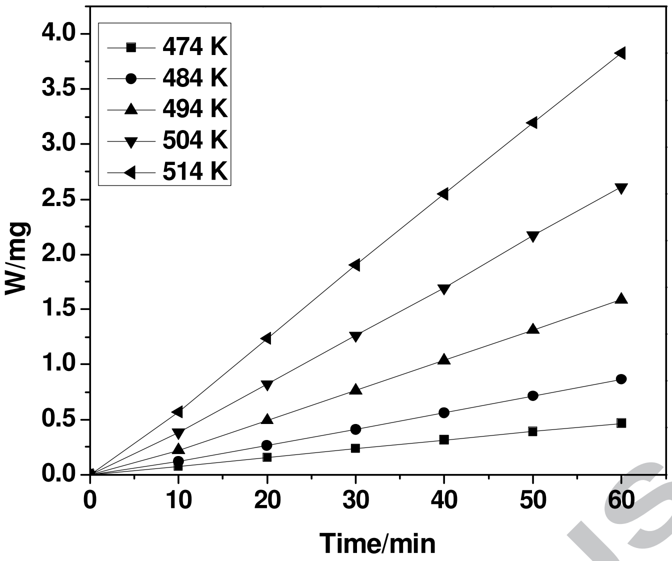

(a)

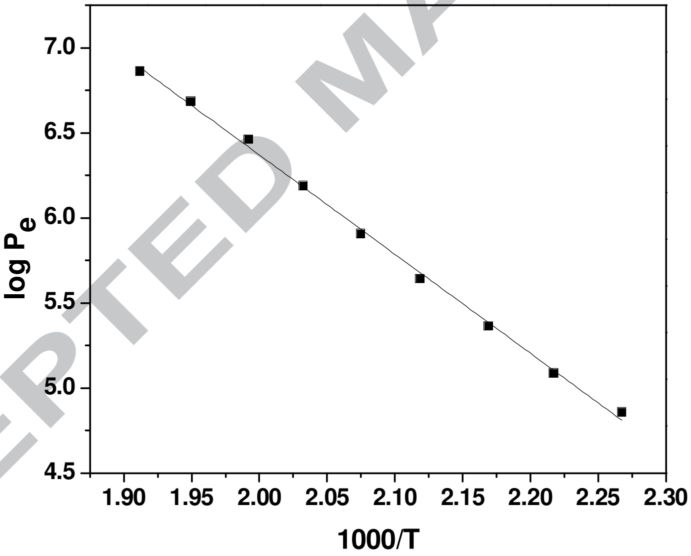

(b)

Fig 5: (a) Mass loss against time isothermal plots and (b) Clausius-Clapeyron plot.

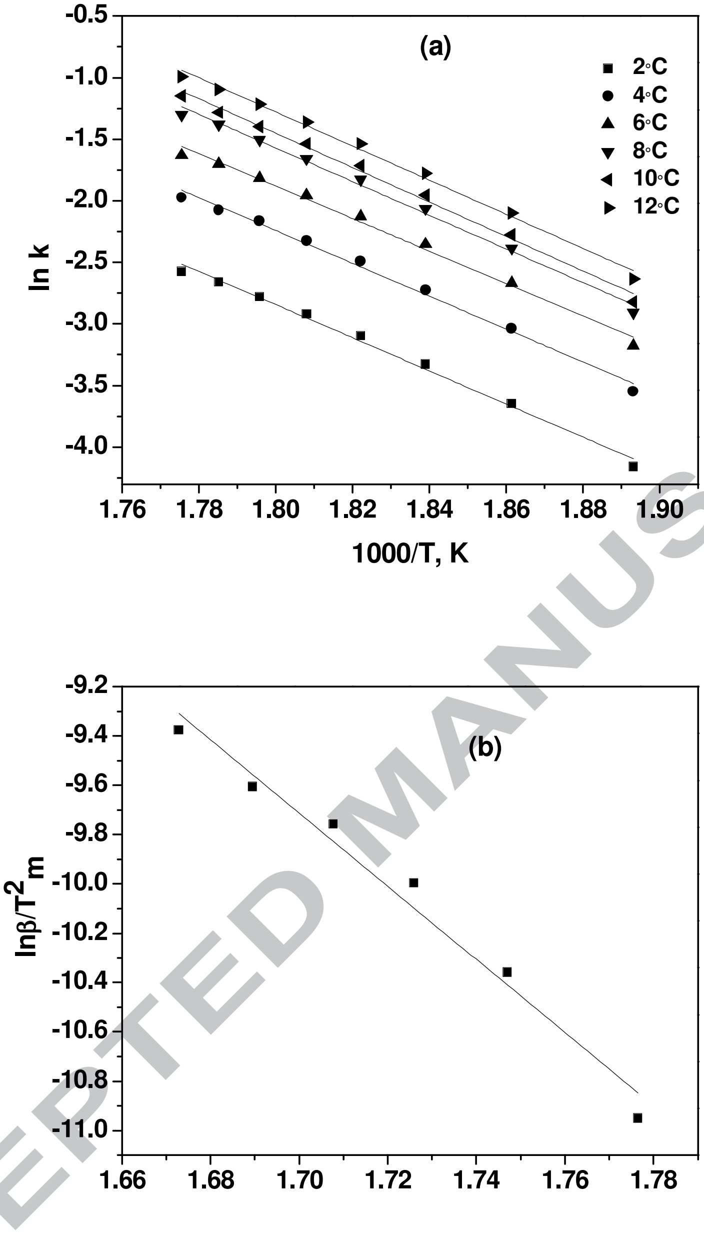
(a)
ln k
1000/T, K
2◦C
4◦C
6◦C
8◦C
10◦C
12◦C
-0.5
-1.0
-1.5
-2.0
-2.5
-3.0
-3.5
-4.0
1.76
1.78
1.80
1.82
1.84
1.86
1.88
1.90
(b)
lnβ/T2m
1000/Tm,K
-9.2
-9.4
-9.6
-9.8
-10.0
-10.2
-10.4
-10.6
-10.8
-11.0
1.66
1.68
1.70
1.72
1.74
1.76
1.78

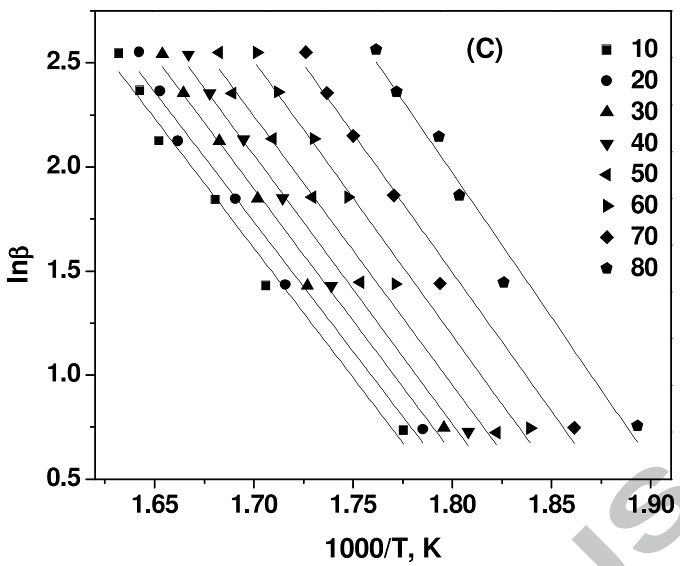
(C)
lnβ
2.5
2.0
1.5
1.0
0.5
1.65
1.70
1.75
1.80
1.85
1.90
1000/T, K
■ 10
● 20
▲ 30
▼ 40
◀ 50
▶ 60
◆ 70
⬟ 80

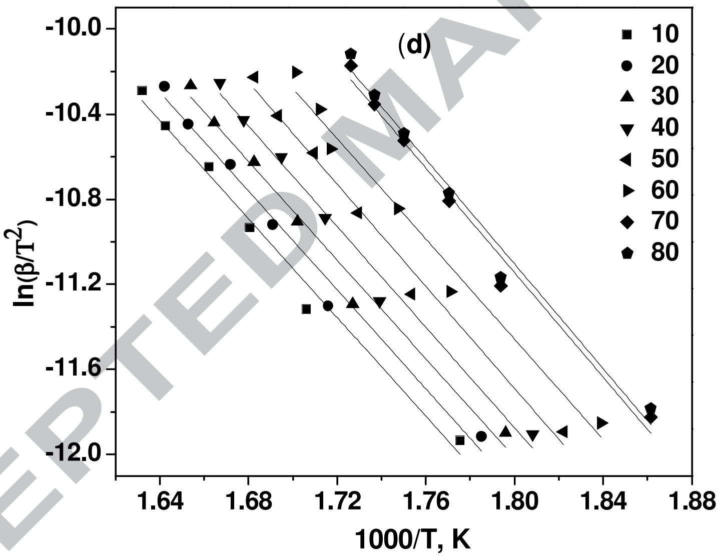
(d)
ln(β/T^2)
-10.0
-10.4
-10.8
-11.2
-11.6
-12.0
1.64
1.68
1.72
1.76
1.80
1.84
1.88
1000/T, K
■ 10
● 20
▲ 30
▼ 40
◀ 50
▶ 60
◆ 70
⬟ 80

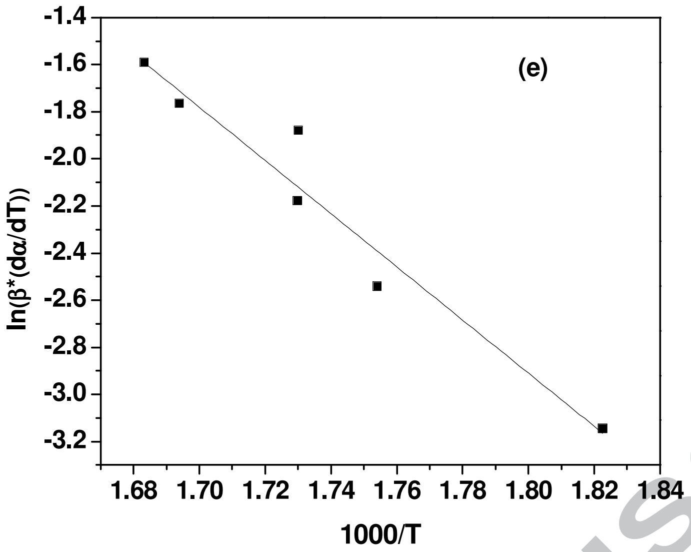

Fig 6: Non-isothermal plots (a) Arrhenius Plots of ln k vs 1/T (b) Kissinger Plot of ln(β/T^2_m) vs 1/T_m (c) Flynn – Wall of ln β vs 1/T (d) Kissinger-Akahira-Sunrose (KAS) Plot of ln(β/T^2) vs 1/T (e) Friedman Plots of lnβ*(dα/dT) vs 1/T of bis(N-isopropylsalicylaldimine)cobalt(II) at different heating rates °C (min^{-1}).

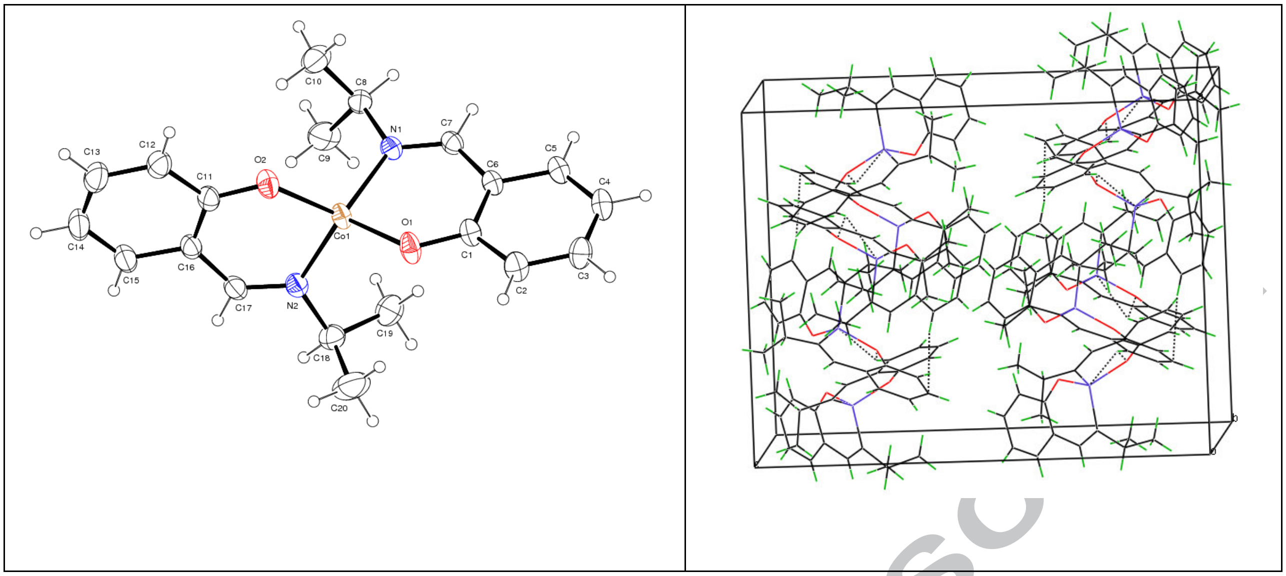

Fig 7: ORTEP and packing diagram of bis(N-isopropylsalicylaldimine)cobalt(II) with 50% probability.

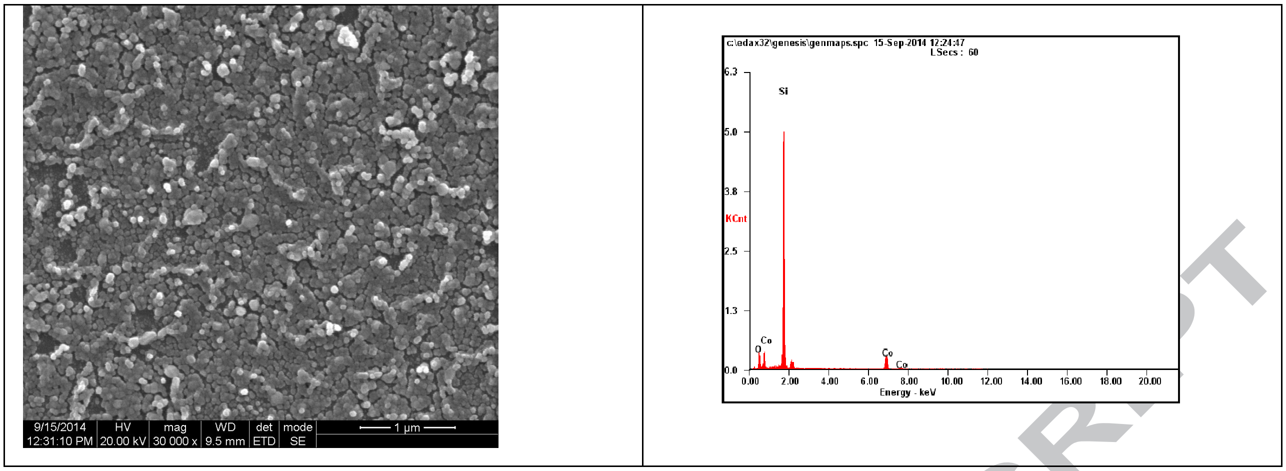

Fig 8: SEM and EDAX images of the cobalt oxide coating obtained on silica substrate using bis(N-isopropylsalicylaldimine)cobalt(II) complex as precursor.

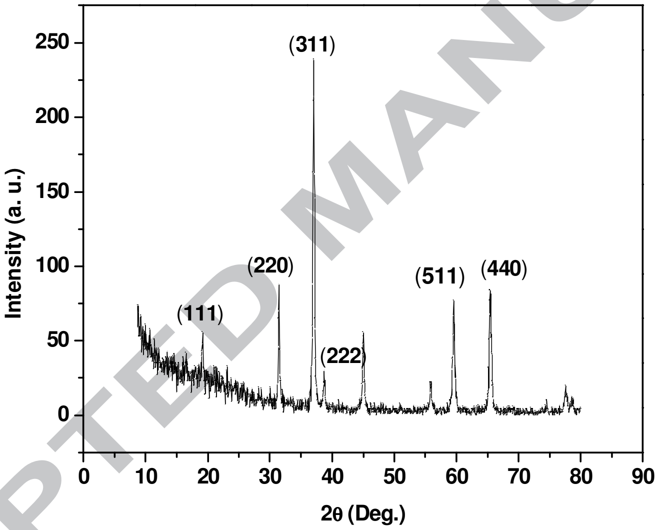

Fig 9: X-ray Diffraction of the powder cobalt oxide collected from the thin film coatings over silica substrate.

Table Titles:

1. Table 1:Non-isothermal sublimation kinetics of bis(N-isopropylsalicylaldimine)cobalt(II)
2. Table 2:Experimental crystal data for bis(N-isopropylsalicylaldimine)cobalt(II).
3. Table 3:Selected interatomic distances (Å) and angles (°) for bis(N-isopropylsalicylaldimine)cobalt(II)

Table 1:

Non-isothermal sublimation kinetics of bis(N-isopropylsalicylaldimine)cobalt(II).

Non-isoconvertional methods	**E_a , $kJmol^{-1}$**
Arrhenius method	111±0.4, 110±0.4, 109±0.4, 113±0.4, 116±0.4 and 115±0.4
Flynn Wall Ozawa method	123±1
Kissinger method	107±0.7
Kissinger-Akahira-Sunrose method	98±0.7
Friedman method	93.8±1.3

Table 2:
Experimental crystal data for bis(N-isopropylsalicylaldimine)cobalt(II).

Empirical Formula	$C_{20}H_{25}CoN_2O_2$
Formulae weight	384.35
Temperature	296(2) K
Crystal System, Space group	Orthorhombic, Pbca
a(Å)	15.1638(7)
b(Å)	13.1829(6)
c(Å)	19.3931(9)
α(°)	90
β(°)	90
γ(°)	90
Volume (Å^3)	3876.7(3)
Z, Calculated density (D_{calc}) (mg/m^3)	Z: 8, 1.317
Absorption coefficient (mm^{-1})	0.900
F(000)	1616
Crystal Size	0.40 x 0.30 x 0.30 mm
Theta range for data collection (°)	2.30 to 29.58
Limiting indices	$-22 \leq h \leq 21$, $-18 \leq K \leq 16$, $-26 \leq l \leq 26$
Reflections collected / unique (R_{int})	71880 / 5399 [R(int) = 0.0317]
Completeness to theta	29.58 99.3 %
Absorption correction	Semi-empirical from equivalents
Max. and min. transmission	0.801 and 0.682
Refinement method	Full-matrix least-squares on F$^{\wedge 2}$
Data/restraints/parameters	5399 / 0 / 230
Goodness-of-fit on F^2	1.110
Final R indices [I > 2σ(I)]	R1 = 0.0345, wR2 = 0.0857
R Indices (all data)	R1 = 0.0629, wR2 = 0.1050
Largest diff. peak and hole	0.360 and -0.356 e.A$^{\wedge -3}$

Table 3:
Selected interatomic distances (Å), angles (°) for bis(N-isopropylsalicylaldimine)cobalt(II).

C(7)-N(1)	1.289(2)	N(1)-C(7)-C(6)	127.55(16)
C(8)-N(1)	1.474(2)	N(1)-C(8)-C(9)	109.85(16)
C(11)-O(2)	1.308(2)	N(1)-C(8)-C(10)	109.89(18)
C(1)-O(1)	1.308(2)	N(2)-C(17)-C(16)	127.71(18)
C(1)-C(2)	1.405(3)	N(2)-C(18)-C(19)	110.13(17)
C(1)-C(6)	1.420(2)	N(2)-C(18)-C(20)	108.27(19)
C(6)-C(7)	1.436(2)	C(7)-N(1)-C(8)	118.00(15
C(7)-N(1)	1.289(2)	C(7)-N(1)-Co(1)	120.59(12)
C(8)-N(1)	1.474(2)	C(8)-N(1)-Co(1)	121.39(12)
C(11)-O(2)	1.308(2)	C(17)-N(2)-Co(1)	120.69(14)
C(11)-C(12)	1.406(3)	C(18)-N(2)-Co(1)	121.95(12)
C(11)-C(16)	1.416(3)	C(1)-O(1)-Co(1)	125.57(11)
C(11)-C(16)	1.416(3)	C(11)-O(2)-Co(1)	125.12(13)
C(16)-C(17)	1.440(3)	O(1)-Co(1)-O(2)	118.43(6)
C(17)-N(2)	1.282(2)	O(1)-Co(1)-N(2)	112.10(7)
C(18)-N(2)	1.484(3)	O(2)-Co(1)-N(2)	96.28(6)
N(1)-Co(1)	1.9979(14)	O(1)-Co(1)-N(1)	96.45(6)
N(2)-Co(1)	1.9868(15)	O(2)-Co(1)-N(1)	112.83(6)
O(1)-Co(1)	1.9020(13)	N(2)-Co(1)-N(1)	122.42(6)
O(2)-Co(1)	1.9082(13)		

Selected geometric parameters (Å, °).

Co(1)—O(2)	1.909 (3)	O2^{i}—Co1—O2	180
Co(1)—O(1)	1.921 (3)	O2^{i}—Co1—O1	87.27 (13)
		O2—Co1—O1	92.73 (13)
		O1—Co1—O1^{i}	180

Graphical Abstract Pictogram

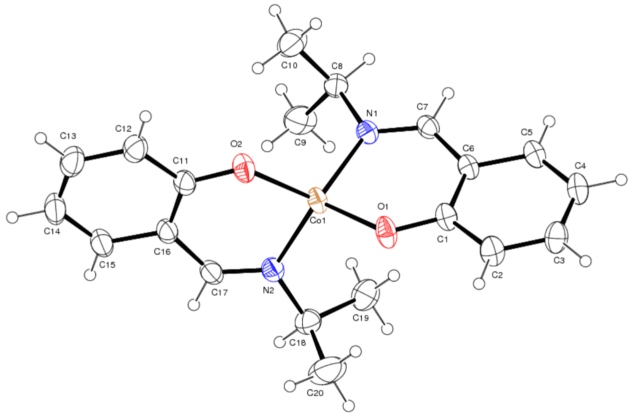

Bis(N-isopropylsalicylaldimine)cobalt(II)

Graphical Abstract Synopsis

A metallo-organic CVD precursor bis(N-isopropylsalicylaldimine)cobalt(II) was synthesized by template method showing orthorhombic space group *Pbac*. In the crystal structure cobalt(II) is surrounded by two Schiff base ligands forming a distorted tetrahedron. The complex was found to be volatile and used in Thermal Chemical Vapor Deposition (TCVD) for the development of nanocrystalline cobalt oxide thin films.